

AD8638/AD8639

FEATURES

- Low offset voltage: 9 μV maximum**
- Offset drift: 0.04 $\mu\text{V}/^\circ\text{C}$ maximum**
- Rail-to-rail output swing**
- 5 V to 16 V single-supply or ± 2.5 V to ± 8 V dual-supply operation**
- High gain: 136 dB typical**
- High CMRR: 133 dB typical**
- High PSRR: 143 dB typical**
- Very low input bias current: 40 pA maximum**
- Low supply current: 1.3 mA maximum**
- AD8639: qualified for automotive applications**

APPLICATIONS

- Pressure and position sensors**
- Strain gage amplifiers**
- Medical instrumentation**
- Thermocouple amplifiers**
- Automotive sensors**
- Precision references**
- Precision current sensing**

GENERAL DESCRIPTION

The AD8638/AD8639 are single and dual wide bandwidth, auto-zero amplifiers featuring rail-to-rail output swing and low noise. These amplifiers have very low offset, drift, and bias current. Operation is fully specified from 5 V to 16 V single supply (± 2.5 V to ± 8 V dual supply).

The AD8638/AD8639 provide benefits previously found only in expensive zero-drift or chopper-stabilized amplifiers. Using the Analog Devices, Inc., topology, these auto-zero amplifiers combine low cost with high accuracy and low noise. No external capacitors are required. In addition, the AD8638/AD8639 greatly reduce the digital switching noise found in most chopper-stabilized amplifiers.

With a typical offset voltage of only 3 μV , drift of 0.01 $\mu\text{V}/^\circ\text{C}$, and noise of 1.2 μV p-p (0.1 Hz to 10 Hz), the AD8638/AD8639 are suited for applications in which error sources cannot be tolerated. Position and pressure sensors, medical equipment, and strain gage amplifiers benefit greatly from nearly zero drift over their operating temperature ranges. Many systems can take advantage of the rail-to-rail output swing provided by the AD8638/AD8639 to maximize signal-to-noise ratio (SNR).

PIN CONFIGURATIONS

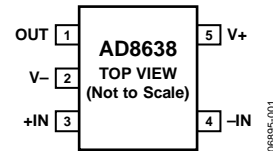


Figure 1. 5-Lead SOT-23 (RJ-5)

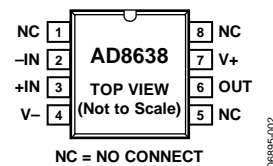
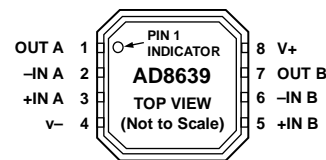


Figure 2. 8-Lead SOIC_N (R-8)



Figure 3. 8-Lead MSOP (RM-8)
8-Lead SOIC_N (R-8)



- NOTES**
1. PIN 4 AND THE EXPOSED PAD MUST BE CONNECTED TO V-.

Figure 4. 8-Lead LFCSP_WD (CP-8-5)

The AD8638/AD8639 are specified for the extended industrial temperature range (-40°C to $+125^\circ\text{C}$). The single AD8638 is available in tiny 5-lead SOT-23 and 8-lead SOIC packages. The dual AD8639 is available in 8-lead MSOP, 8-lead SOIC, and 8-lead LFCSP packages. See the Ordering Guide for automotive grades.

The AD8638/AD8639 are members of a growing series of auto-zero op amps offered by Analog Devices (see Table 1).

Table 1. Auto-Zero Op Amps

Supply	2.7 V to 5 V	2.7 V to 5 V Low Power	5 V to 16 V
Single	AD8628	AD8538	AD8638
Dual	AD8629	AD8539	AD8639
Quad	AD8630		

Rev. F

Information furnished by Analog Devices is believed to be accurate and reliable. However, no responsibility is assumed by Analog Devices for its use, nor for any infringements of patents or other rights of third parties that may result from its use. Specifications subject to change without notice. No license is granted by implication or otherwise under any patent or patent rights of Analog Devices. Trademarks and registered trademarks are the property of their respective owners.

TABLE OF CONTENTS

Features	1	Theory of Operation	14
Applications.....	1	1/f Noise.....	14
General Description	1	Input Voltage Range.....	14
Pin Configurations	1	Output Phase Reversal.....	14
Revision History	2	Overload Recovery Time	14
Specifications.....	3	Infrared Sensors.....	15
Electrical Characteristics—5 V Operation.....	3	Precision Current Shunt Sensor	15
Electrical Characteristics—16 V Operation	4	Output Amplifier for High Precision DACs.....	15
Absolute Maximum Ratings.....	5	Outline Dimensions	16
Thermal Resistance	5	Ordering Guide	18
ESD Caution.....	5	Automotive Products.....	18
Typical Performance Characteristics	6		

REVISION HISTORY

6/10—Rev. E to Rev. F

Changes to Features Section and General Description Section .	1
Updated Outline Dimensions	16
Changes to Ordering Guide	18
Added Automotive Products Section	18

6/09—Rev. D to Rev. E

Changes to Figure 4.....	1
Changes to Endnote 1 and Endnote 2, Table 4.....	5
Changes to Input Voltage Range Section	14
Updated Outline Dimensions	16
Changes to Ordering Guide	18

12/08—Rev. C to Rev. D

Changes to Endnote 1, Table 4.....	5
Changes to Ordering Guide	28

5/08—Rev. B to Rev. C

Added LFCSP_WD Package	Universal
Inserted Figure 4; Renumbered Sequentially.....	1
Changes to Layout	1
Changes to General Description	1
Changes to Offset Voltage Drift for All Packages Except SOT-23 Parameter in Table 2.....	3
Changes to Table 5.....	5
Updated Outline Dimensions	16
Changes to Ordering Guide	17

4/08—Rev. A to Rev. B

Added AD8639	Universal
Added 8-lead MSOP Package	Universal
Changes to Features	1
Changes to General Description	1
Changes Table 2	3
Changes to Table 3.....	4
Changes to Table 4, Added Endnote 1 and Endnote 2.....	5
Changes to Figure 4 through Figure 9	6
Changes to Figure 11, Figure 12, Figure 14, and Figure 15.....	7
Changes to Figure 16 through Figure 27.....	8
Changes to Figure 28 through Figure 33.....	10
Changes to Figure 34 through Figure 39.....	11
Changes to Figure 41 and Figure 44.....	12
Inserted Figure 46, Figure 47, Figure 49, and Figure 50; Renumbered Sequentially	13
Changes to Figure 51, Figure 52, and Figure 53.....	15
Updated Outline Dimensions.....	16
Changes to Ordering Guide	17

11/07—Rev. 0 to Rev. A

Change to Large Signal Voltage Gain Specification.....	4
--	---

11/07—Revision 0: Initial Version

SPECIFICATIONS

ELECTRICAL CHARACTERISTICS—5 V OPERATION

$V_{SY} = 5\text{ V}$, $V_{CM} = V_{SY}/2$, $T_A = 25^\circ\text{C}$, unless otherwise noted.

Table 2.

Parameter	Symbol	Conditions	Min	Typ	Max	Unit
INPUT CHARACTERISTICS						
Offset Voltage	V_{OS}	$-40^\circ\text{C} \leq T_A \leq +125^\circ\text{C}$		3	9	μV
		$-0.1\text{ V} \leq V_{CM} \leq +3.0\text{ V}$			23	μV
		$-40^\circ\text{C} \leq T_A \leq +125^\circ\text{C}$		3	9	μV
		$-40^\circ\text{C} \leq T_A \leq +125^\circ\text{C}$			23	μV
Input Bias Current	I_B	$-40^\circ\text{C} \leq T_A \leq +85^\circ\text{C}$		1.5	40	pA
		$-40^\circ\text{C} \leq T_A \leq +125^\circ\text{C}$		7	40	pA
		$-40^\circ\text{C} \leq T_A \leq +125^\circ\text{C}$		45	105	pA
Input Offset Current	I_{OS}	$-40^\circ\text{C} \leq T_A \leq +85^\circ\text{C}$		7	40	pA
		$-40^\circ\text{C} \leq T_A \leq +125^\circ\text{C}$		7	40	pA
		$-40^\circ\text{C} \leq T_A \leq +125^\circ\text{C}$		16.5	60	pA
Input Voltage Range		$-40^\circ\text{C} \leq T_A \leq +125^\circ\text{C}$	-0.1		+3	V
Common-Mode Rejection Ratio	CMRR	$V_{CM} = 0\text{ V to }3\text{ V}$	118	133		dB
		$-40^\circ\text{C} \leq T_A \leq +125^\circ\text{C}$	118			dB
Large Signal Voltage Gain	A_{VO}	$R_L = 10\text{ k}\Omega$, $V_O = 0.5\text{ V to }4.5\text{ V}$	120	136		dB
		$-40^\circ\text{C} \leq T_A \leq +125^\circ\text{C}$	119			dB
Offset Voltage Drift for All Packages Except SOT-23	$\Delta V_{OS}/\Delta T$	$-40^\circ\text{C} \leq T_A \leq +125^\circ\text{C}$		0.01	0.06	$\mu\text{V}/^\circ\text{C}$
Offset Voltage Drift for SOT-23	$\Delta V_{OS}/\Delta T$	$-40^\circ\text{C} \leq T_A \leq +125^\circ\text{C}$		0.04	0.15	$\mu\text{V}/^\circ\text{C}$
Input Resistance	R_{IN}			22.5		$\text{T}\Omega$
Input Capacitance, Differential Mode	C_{INDM}			4		pF
Input Capacitance, Common Mode	C_{INCM}			1.7		pF
OUTPUT CHARACTERISTICS						
Output Voltage High	V_{OH}	$R_L = 10\text{ k}\Omega$ to V_{CM}	4.97	4.985		V
		$-40^\circ\text{C} \leq T_A \leq +125^\circ\text{C}$	4.97			V
		$R_L = 2\text{ k}\Omega$ to V_{CM}	4.90	4.93		V
		$-40^\circ\text{C} \leq T_A \leq +125^\circ\text{C}$	4.86			V
Output Voltage Low	V_{OL}	$R_L = 10\text{ k}\Omega$ to V_{CM}		7.5	10	mV
		$-40^\circ\text{C} \leq T_A \leq +125^\circ\text{C}$			15	mV
		$R_L = 2\text{ k}\Omega$ to V_{CM}		32	40	mV
		$-40^\circ\text{C} \leq T_A \leq +125^\circ\text{C}$			55	mV
Short-Circuit Current	I_{SC}	$T_A = 25^\circ\text{C}$		± 19		mA
Closed-Loop Output Impedance	Z_{OUT}	$f = 100\text{ kHz}$, $A_V = 1$		4.2		Ω
POWER SUPPLY						
Power Supply Rejection Ratio	PSRR	$V_{SY} = 4.5\text{ V to }16\text{ V}$	127	143		dB
		$-40^\circ\text{C} \leq T_A \leq +125^\circ\text{C}$	125			dB
Supply Current per Amplifier	I_{SY}	$I_O = 0\text{ mA}$		1.0	1.3	mA
		$-40^\circ\text{C} \leq T_A \leq +125^\circ\text{C}$			1.5	mA
DYNAMIC PERFORMANCE						
Slew Rate	SR	$R_L = 10\text{ k}\Omega$, $C_L = 20\text{ pF}$, $A_V = 1$		2.5		$\text{V}/\mu\text{s}$
Settling Time to 0.1%	t_S	$V_{IN} = 2\text{ V step}$, $C_L = 20\text{ pF}$, $R_L = 1\text{ k}\Omega$, $A_V = 1$		3		μs
Overload Recovery Time				50		μs
Gain Bandwidth Product	GBP	$R_L = 2\text{ k}\Omega$, $C_L = 20\text{ pF}$, $A_V = 1$		1.35		MHz
Phase Margin	Φ_M	$R_L = 2\text{ k}\Omega$, $C_L = 20\text{ pF}$, $A_V = 1$		70		Degrees
NOISE PERFORMANCE						
Voltage Noise	e_n p-p	0.1 Hz to 10 Hz		1.2		$\mu\text{V p-p}$
Voltage Noise Density	e_n	$f = 1\text{ kHz}$		60		$\text{nV}/\sqrt{\text{Hz}}$

AD8638/AD8639

ELECTRICAL CHARACTERISTICS—16 V OPERATION

$V_{SY} = 16\text{ V}$, $V_{CM} = V_{SY}/2$, $T_A = 25^\circ\text{C}$, unless otherwise noted.

Table 3.

Parameter	Symbol	Conditions	Min	Typ	Max	Unit
INPUT CHARACTERISTICS						
Offset Voltage	V_{OS}	$-40^\circ\text{C} \leq T_A \leq +125^\circ\text{C}$		3	9	μV
		$-0.1\text{ V} \leq V_{CM} \leq +14\text{ V}$		3	9	μV
		$-40^\circ\text{C} \leq T_A \leq +125^\circ\text{C}$				23
Input Bias Current	I_B	$-40^\circ\text{C} \leq T_A \leq +85^\circ\text{C}$		1	75	pA
		$-40^\circ\text{C} \leq T_A \leq +125^\circ\text{C}$		4	75	pA
		$-40^\circ\text{C} \leq T_A \leq +125^\circ\text{C}$		85	250	pA
Input Offset Current	I_{OS}	$-40^\circ\text{C} \leq T_A \leq +85^\circ\text{C}$		20	70	pA
		$-40^\circ\text{C} \leq T_A \leq +125^\circ\text{C}$		20	75	pA
		$-40^\circ\text{C} \leq T_A \leq +125^\circ\text{C}$		50	150	pA
Input Voltage Range		$-40^\circ\text{C} \leq T_A \leq +125^\circ\text{C}$	-0.1		+14	V
Common-Mode Rejection Ratio	CMRR	$V_{CM} = 0\text{ V to }14\text{ V}$	127	142		dB
		$-40^\circ\text{C} \leq T_A \leq +125^\circ\text{C}$	127			dB
Large Signal Voltage Gain	A_{VO}	$R_L = 10\text{ k}\Omega$, $V_O = 0.5\text{ V to }15.5\text{ V}$	130	147		dB
		$-40^\circ\text{C} \leq T_A \leq +125^\circ\text{C}$	130			dB
Offset Voltage Drift for All Packages Except SOT-23	$\Delta V_{OS}/\Delta T$	$-40^\circ\text{C} \leq T_A \leq +125^\circ\text{C}$		0.03	0.06	$\mu\text{V}/^\circ\text{C}$
Offset Voltage Drift for SOT-23	$\Delta V_{OS}/\Delta T$	$-40^\circ\text{C} \leq T_A \leq +125^\circ\text{C}$		0.04	0.15	$\mu\text{V}/^\circ\text{C}$
Input Resistance	R_{IN}			22.5		$\text{T}\Omega$
Input Capacitance, Differential Mode	C_{INDM}			4		pF
Input Capacitance, Common Mode	C_{INCM}			1.7		pF
OUTPUT CHARACTERISTICS						
Output Voltage High	V_{OH}	$R_L = 10\text{ k}\Omega$ to V_{CM}	15.94	15.96		V
		$-40^\circ\text{C} \leq T_A \leq +125^\circ\text{C}$	15.93			V
		$R_L = 2\text{ k}\Omega$ to V_{CM}	15.77	15.82		V
		$-40^\circ\text{C} \leq T_A \leq +125^\circ\text{C}$	15.70			V
Output Voltage Low	V_{OL}	$R_L = 10\text{ k}\Omega$ to V_{CM}		30	40	mV
		$-40^\circ\text{C} \leq T_A \leq +125^\circ\text{C}$			60	mV
		$R_L = 2\text{ k}\Omega$ to V_{CM}		120	140	mV
		$-40^\circ\text{C} \leq T_A \leq +125^\circ\text{C}$			200	mV
Short-Circuit Current	I_{SC}	$T_A = 25^\circ\text{C}$		± 37		mA
Closed-Loop Output Impedance	Z_{OUT}	$f = 100\text{ kHz}$, $A_V = 1$		3.0		Ω
POWER SUPPLY						
Power Supply Rejection Ratio	PSRR	$V_{SY} = 4.5\text{ V to }16\text{ V}$	127	143		dB
		$-40^\circ\text{C} \leq T_A \leq +125^\circ\text{C}$	125			dB
Supply Current per Amplifier	I_{SY}	$I_O = 0\text{ mA}$		1.25	1.5	mA
		$-40^\circ\text{C} \leq T_A \leq +125^\circ\text{C}$			1.7	mA
DYNAMIC PERFORMANCE						
Slew Rate	SR	$R_L = 10\text{ k}\Omega$, $C_L = 20\text{ pF}$, $A_V = 1$		2		$\text{V}/\mu\text{s}$
Settling Time to 0.1%	t_s	$V_{IN} = 4\text{ V step}$, $C_L = 20\text{ pF}$, $R_L = 1\text{ k}\Omega$, $A_V = 1$		4		μs
Overload Recovery Time				50		μs
Gain Bandwidth Product	GBP	$R_L = 2\text{ k}\Omega$, $C_L = 20\text{ pF}$, $A_V = 1$		1.5		MHz
Phase Margin	Φ_M	$R_L = 2\text{ k}\Omega$, $C_L = 20\text{ pF}$, $A_V = 1$		74		Degrees
NOISE PERFORMANCE						
Voltage Noise	e_n p-p	0.1 Hz to 10 Hz		1.2		$\mu\text{V p-p}$
Voltage Noise Density	e_n	$f = 1\text{ kHz}$		60		$\text{nV}/\sqrt{\text{Hz}}$

ABSOLUTE MAXIMUM RATINGS

Table 4.

Parameter	Rating
Supply Voltage	16 V
Input Voltage	GND – 0.3 V to $V_{SY+} + 0.3$ V
Input Current ¹	±10 mA
Differential Input Voltage ²	± V_{SY}
Output Short-Circuit Duration to GND	Indefinite
Storage Temperature Range	–65°C to +150°C
Operating Temperature Range	–40°C to +125°C
Junction Temperature Range	–65°C to +150°C
Lead Temperature (Soldering, 60 sec)	300°C

¹ Input pins have clamp diodes to the supply pins. Input current should be limited to 10 mA or less whenever input signals exceed either power supply rail by 0.3 V.

² Inputs are protected against high differential voltages by internal 1 k Ω series resistors and back-to-back diode-connected N-MOSFETs (with a typical V_T of 1.25 V for V_{CM} of 0 V).

Stresses above those listed under Absolute Maximum Ratings may cause permanent damage to the device. This is a stress rating only; functional operation of the device at these or any other conditions above those indicated in the operational section of this specification is not implied. Exposure to absolute maximum rating conditions for extended periods may affect device reliability.

THERMAL RESISTANCE

Table 5. Thermal Resistance

Package Type	θ_{JA} ¹	θ_{JC}	Unit
5-Lead SOT-23 (RJ-5)	230	146	°C/W
8-Lead SOIC_N (R-8)	158	43	°C/W
8-Lead MSOP (RM-8)	206	44	°C/W
8-Lead LFCSP_WD (CP-8-5) ²	75	18	°C/W

¹ θ_{JA} is specified for the worst-case conditions, that is, a device soldered in a circuit board for surface-mount packages. This was measured using a standard two-layer board.

² Exposed pad is soldered to the application board.

ESD CAUTION



ESD (electrostatic discharge) sensitive device.

Charged devices and circuit boards can discharge without detection. Although this product features patented or proprietary protection circuitry, damage may occur on devices subjected to high energy ESD. Therefore, proper ESD precautions should be taken to avoid performance degradation or loss of functionality.

TYPICAL PERFORMANCE CHARACTERISTICS

$T_A = 25^\circ\text{C}$, unless otherwise noted.

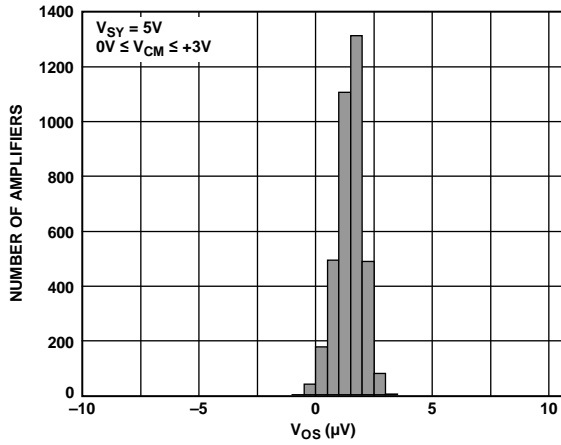


Figure 5. Input Offset Voltage Distribution

06895-003

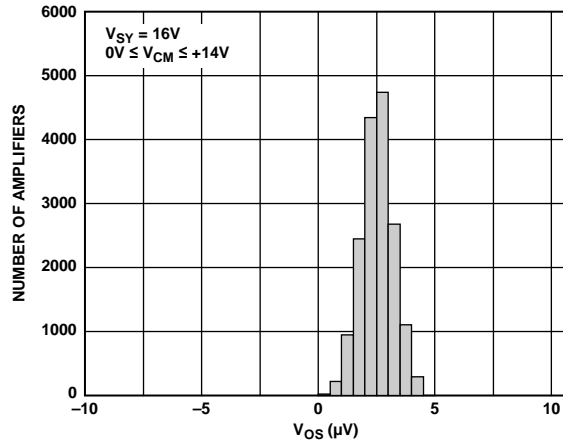


Figure 8. Input Offset Voltage Distribution

06895-006

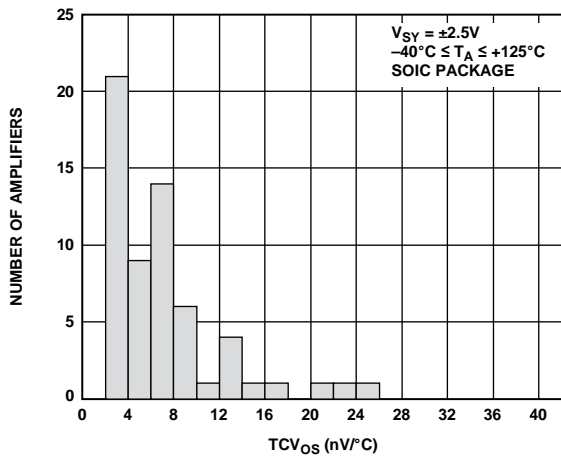


Figure 6. Input Offset Voltage Drift Distribution

06895-004

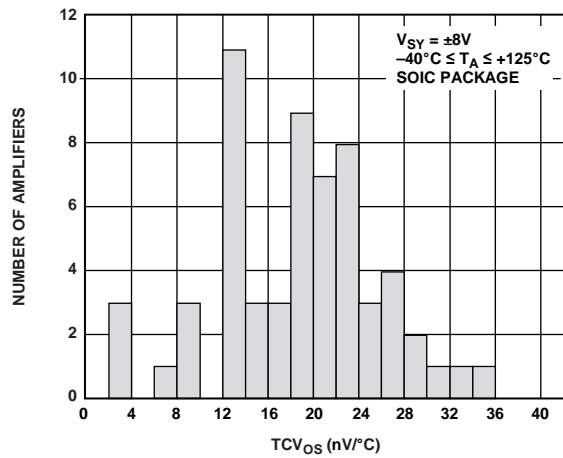


Figure 9. Input Offset Voltage Drift Distribution

06895-007

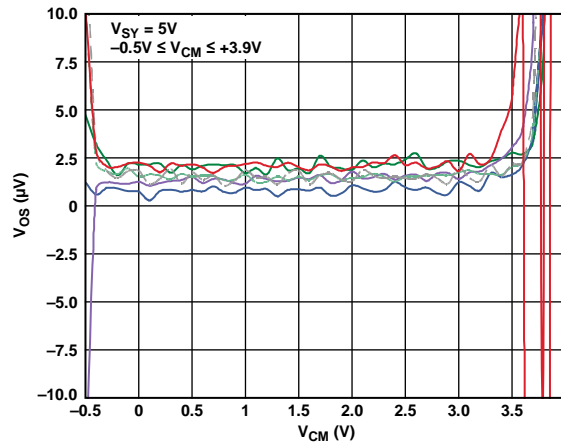


Figure 7. Input Offset Voltage vs. Common-Mode Voltage

06895-005

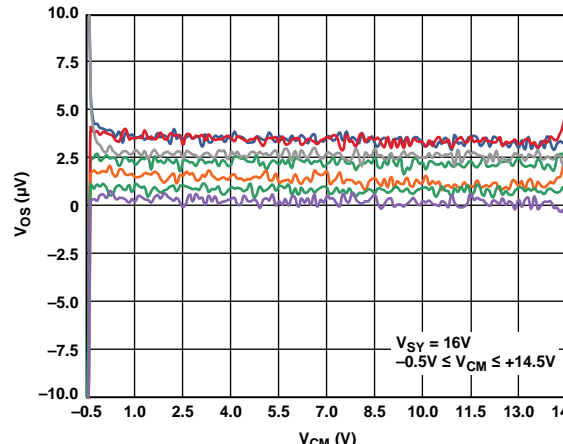


Figure 10. Input Offset Voltage vs. Common-Mode Voltage

06895-008

$T_A = 25^\circ\text{C}$, unless otherwise noted.

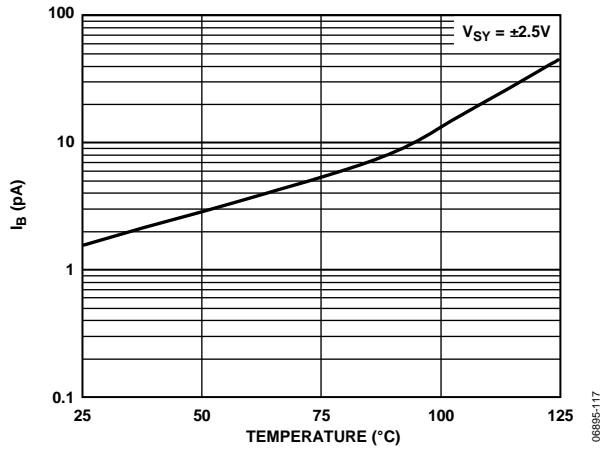


Figure 11. Input Bias Current vs. Temperature

06895-117

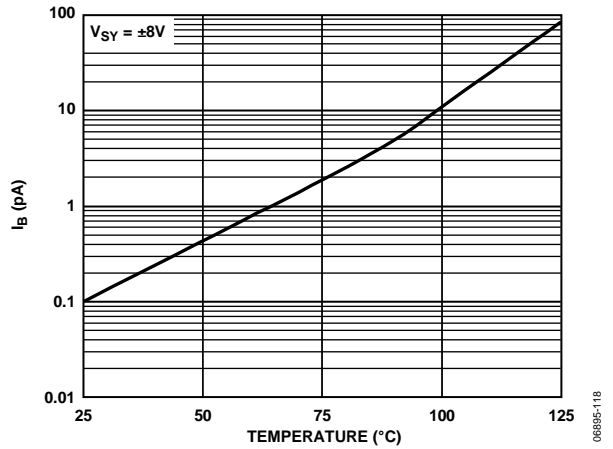


Figure 14. Input Bias Current vs. Temperature

06895-118

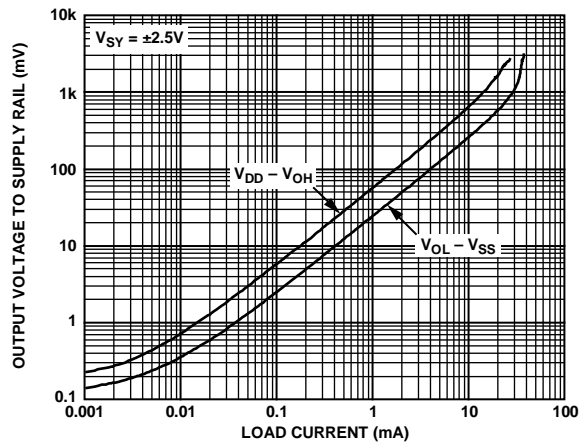


Figure 12. Output Voltage to Supply Rail vs. Load Current

06895-009

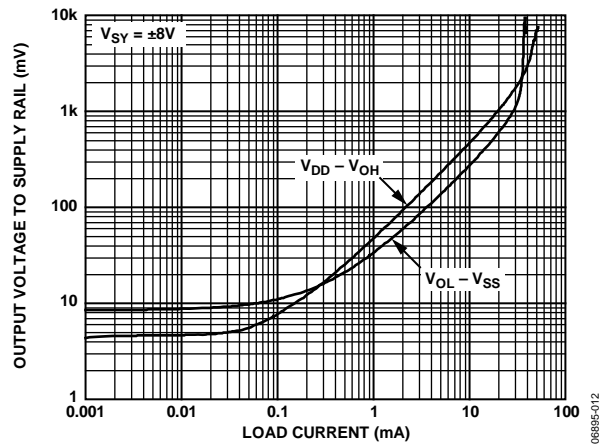


Figure 15. Output Voltage to Supply Rail vs. Load Current

06895-012

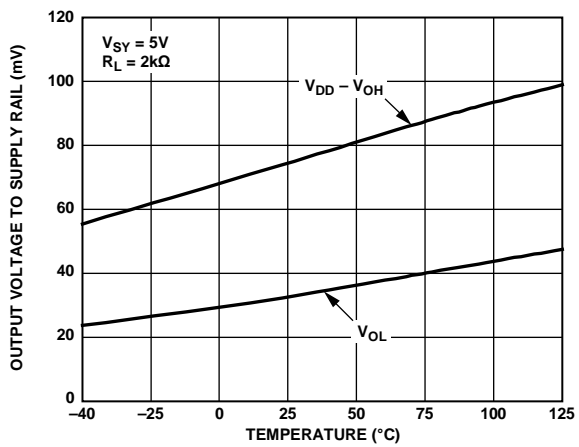


Figure 13. Output Voltage to Supply Rail vs. Temperature

06895-010

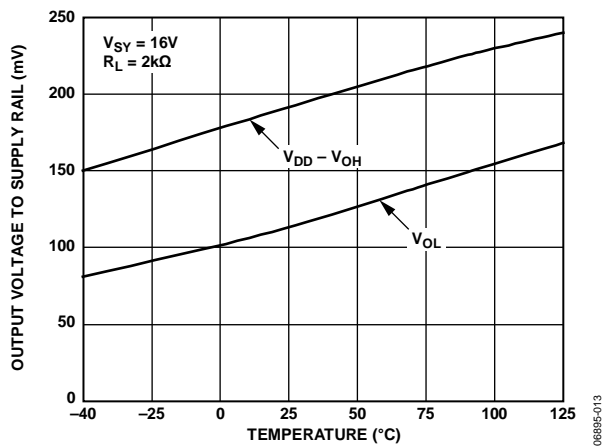


Figure 16. Output Voltage to Supply Rail vs. Temperature

06895-013

AD8638/AD8639

$T_A = 25^\circ\text{C}$, unless otherwise noted.

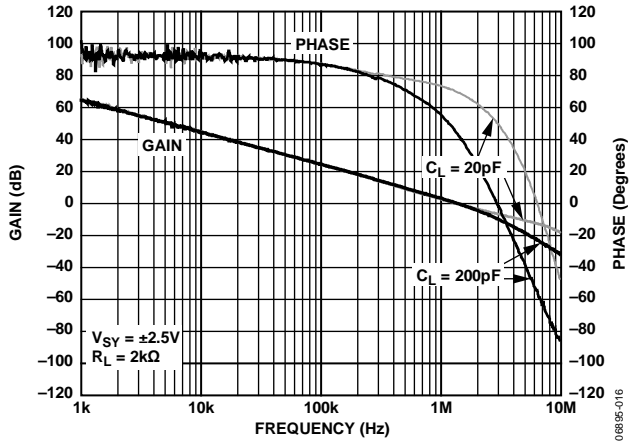


Figure 17. Open-Loop Gain and Phase vs. Frequency

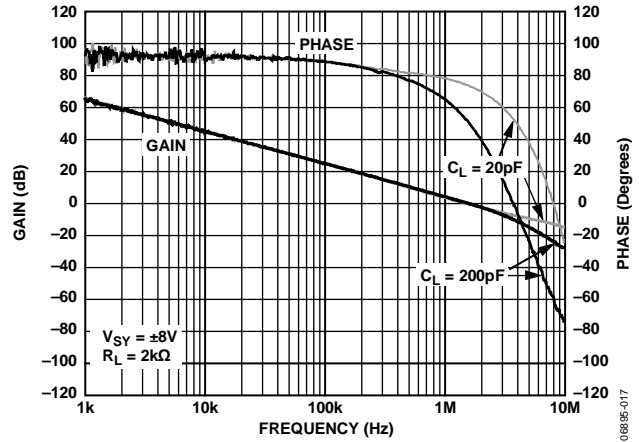


Figure 20. Open-Loop Gain and Phase vs. Frequency

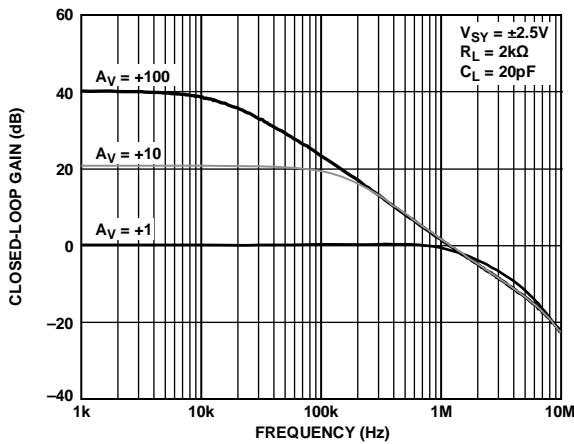


Figure 18. Closed-Loop Gain vs. Frequency

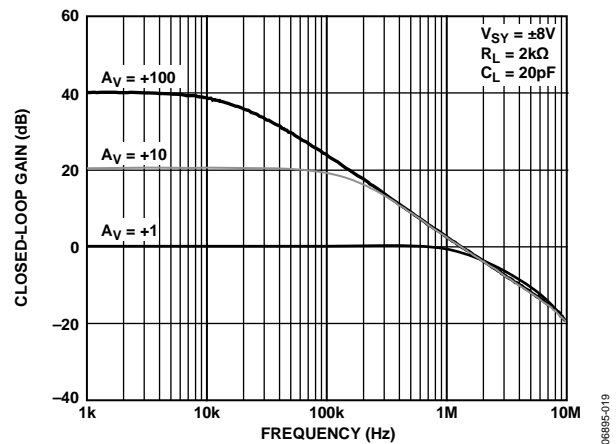


Figure 21. Closed-Loop Gain vs. Frequency

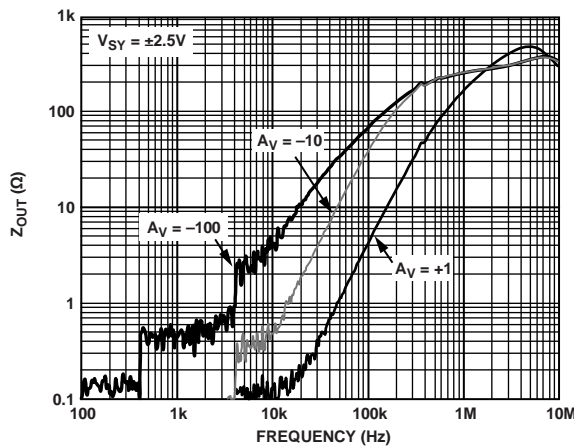


Figure 19. Output Impedance vs. Frequency

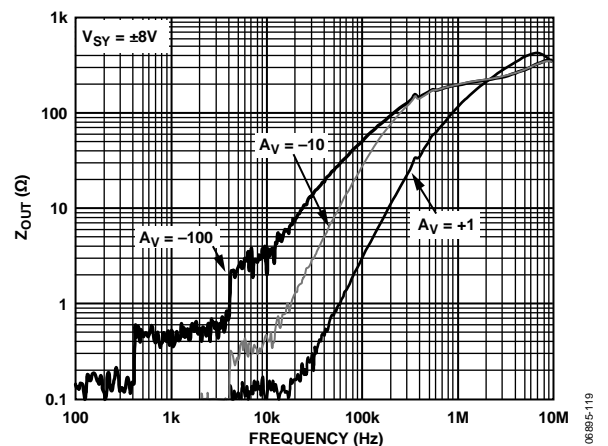


Figure 22. Output Impedance vs. Frequency

$T_A = 25^\circ\text{C}$, unless otherwise noted.

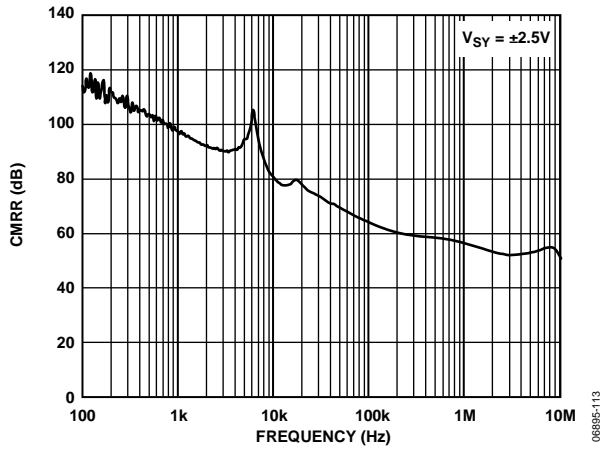


Figure 23. CMRR vs. Frequency

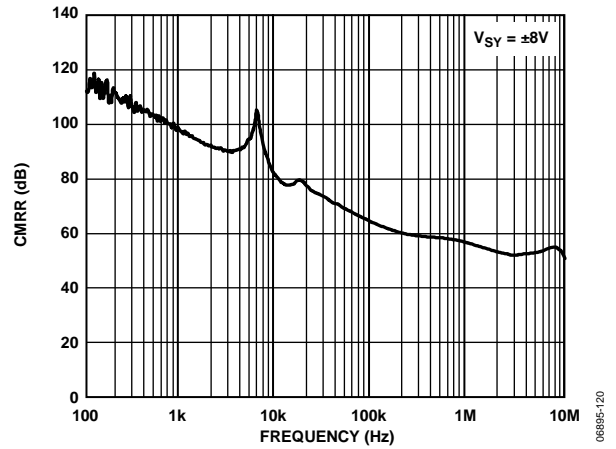


Figure 26. CMRR vs. Frequency

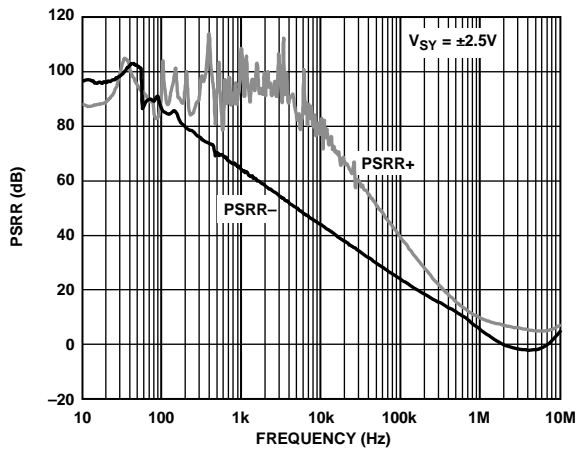


Figure 24. PSRR vs. Frequency

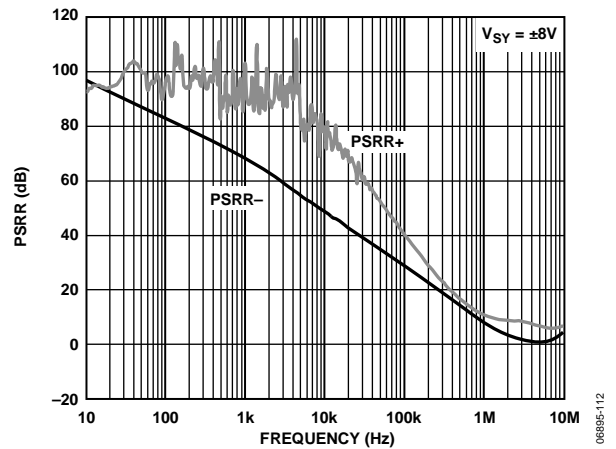


Figure 27. PSRR vs. Frequency

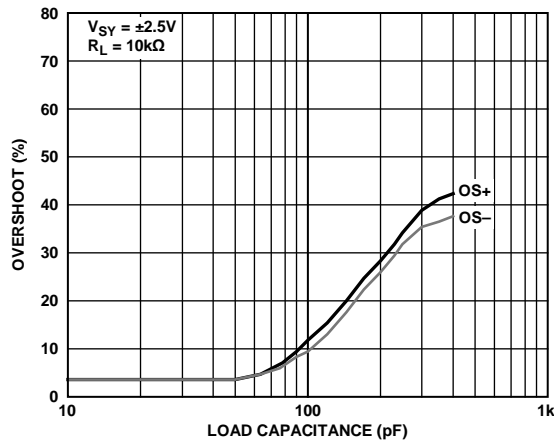


Figure 25. Small Signal Overshoot vs. Load Capacitance

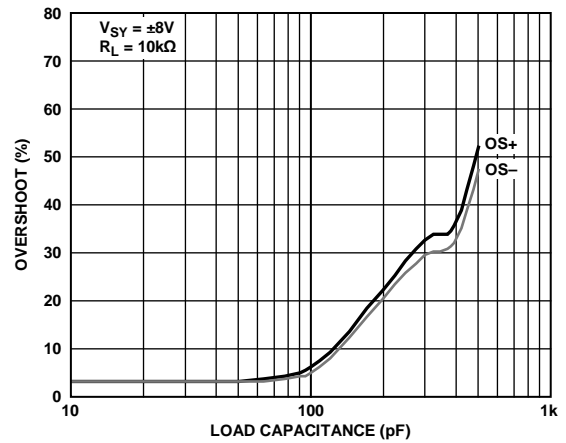


Figure 28. Small Signal Overshoot vs. Load Capacitance

AD8638/AD8639

$T_A = 25^\circ\text{C}$, unless otherwise noted.

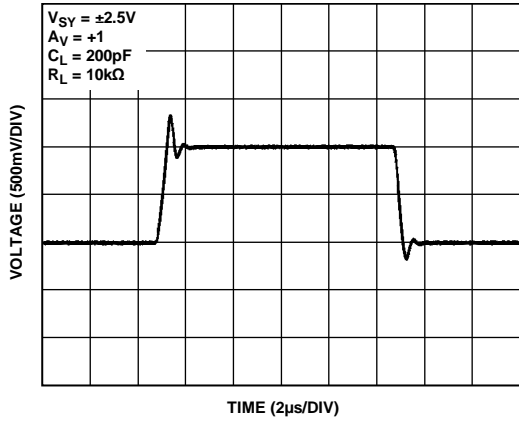


Figure 29. Large Signal Transient Response

068895-101

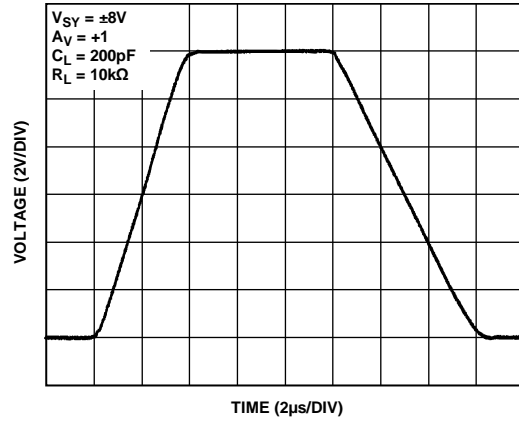


Figure 32. Large Signal Transient Response

068895-102

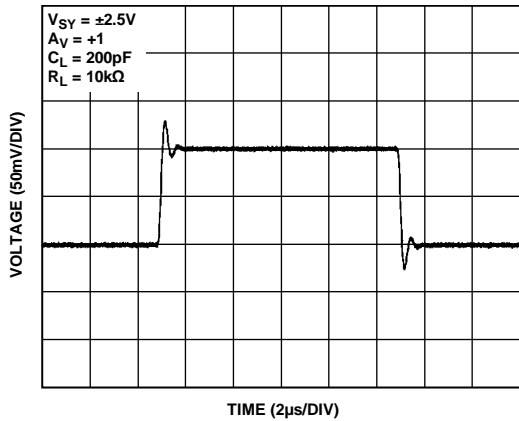


Figure 30. Small Signal Transient Response

068895-103

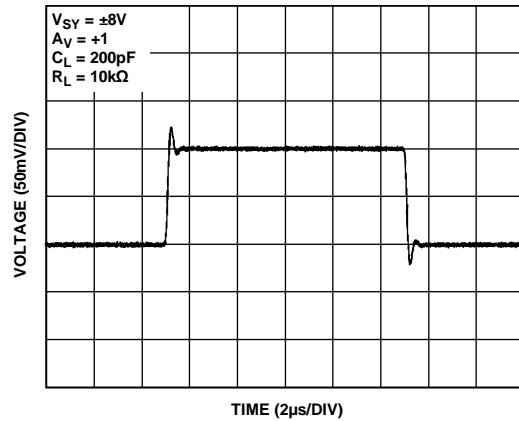


Figure 33. Small Signal Transient Response

068895-104

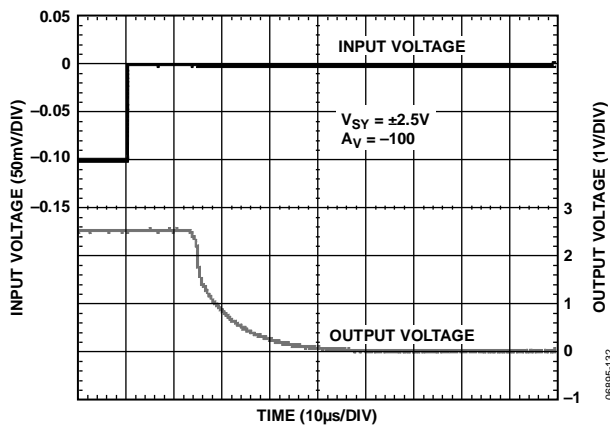


Figure 31. Negative Overload Recovery

068895-132

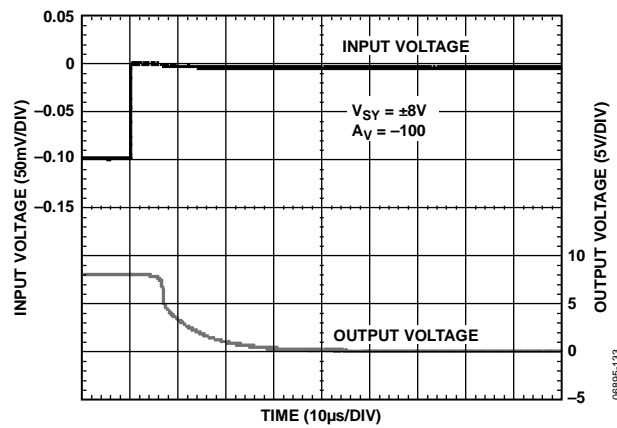


Figure 34. Negative Overload Recovery

068895-133

$T_A = 25^\circ\text{C}$, unless otherwise noted.

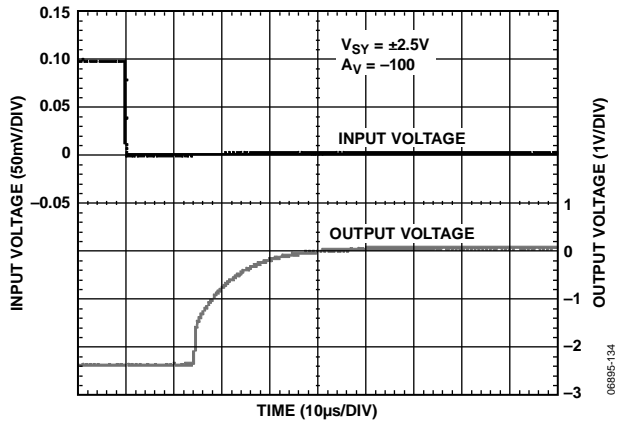


Figure 35. Positive Overload Recovery

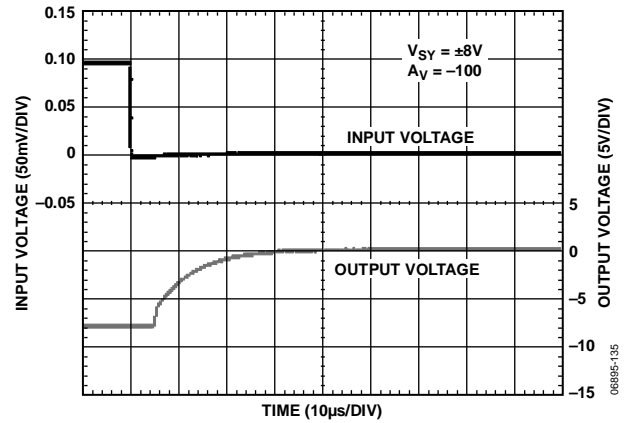


Figure 38. Positive Overload Recovery

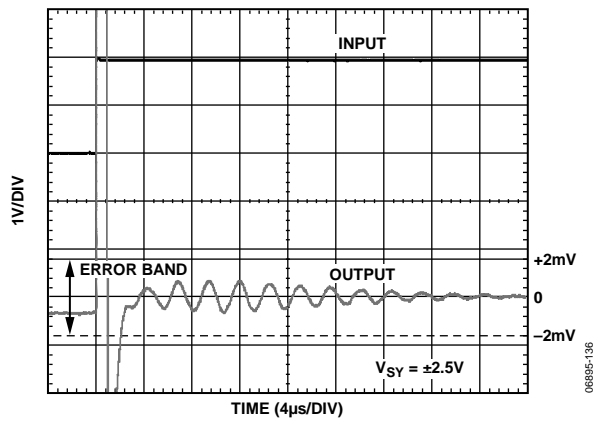


Figure 36. Positive Settling Time to 0.1%

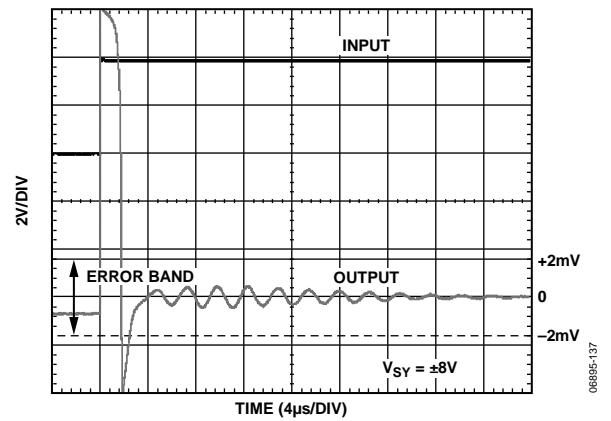


Figure 39. Positive Settling Time to 0.1%

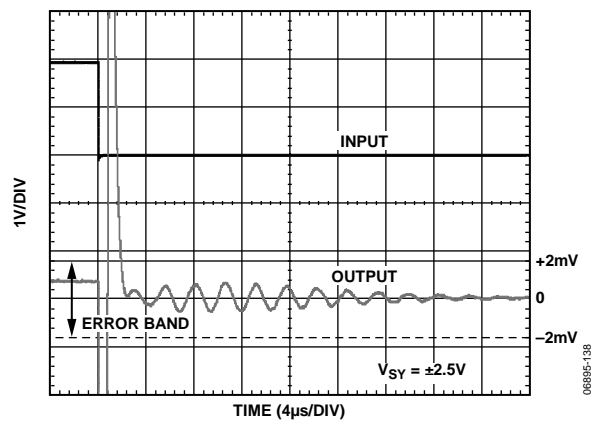


Figure 37. Negative Settling Time to 0.1%

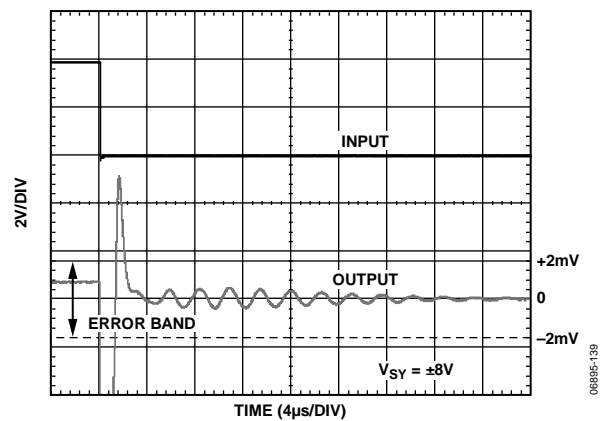


Figure 40. Negative Settling Time to 0.1%

AD8638/AD8639

$T_A = 25^\circ\text{C}$, unless otherwise noted.

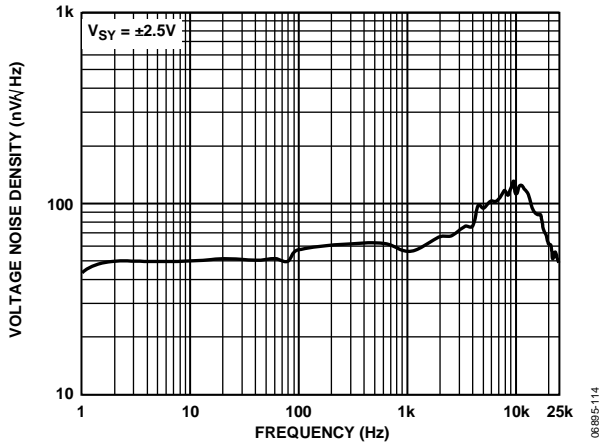


Figure 41. Voltage Noise Density vs. Frequency

06895-114

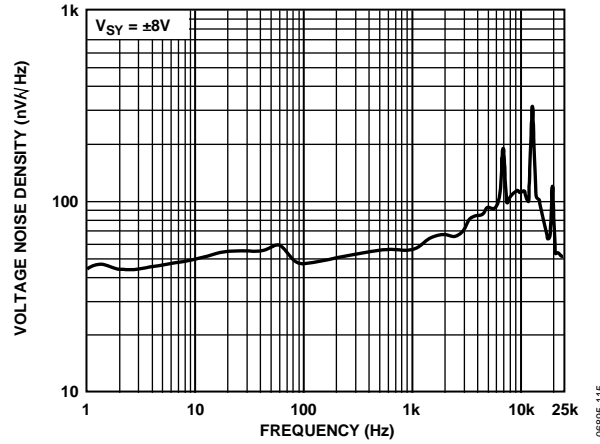


Figure 44. Voltage Noise Density vs. Frequency

06895-115

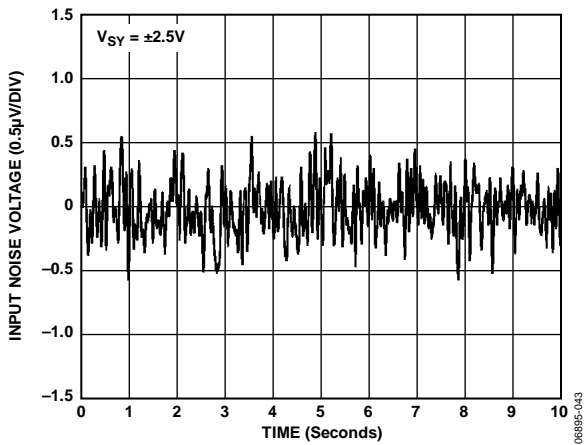


Figure 42. 0.1 Hz to 10 Hz Noise

06895-043

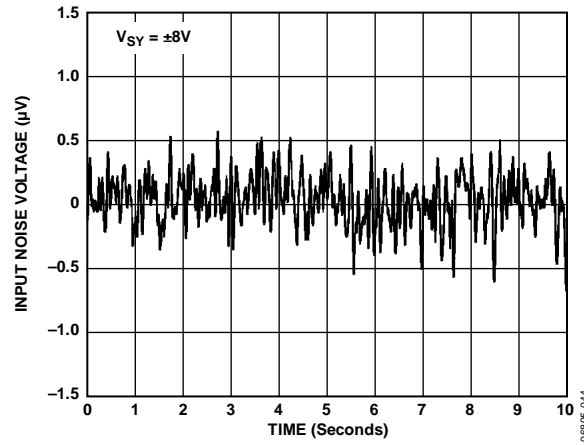


Figure 45. 0.1 Hz to 10 Hz Noise

06895-044

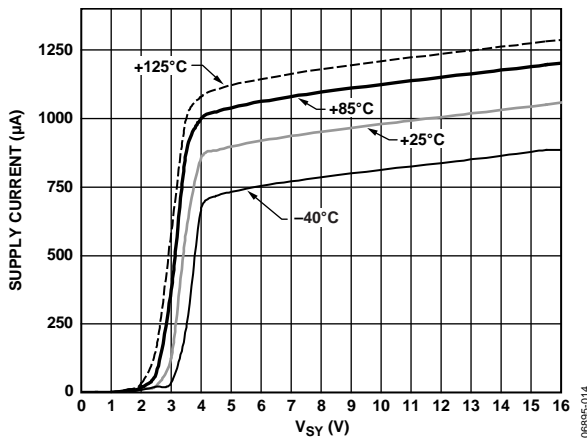


Figure 43. Supply Current vs. Supply Voltage

06895-014

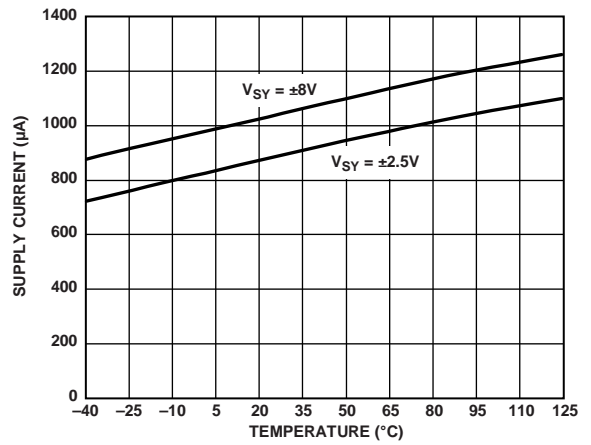


Figure 46. Supply Current vs. Temperature

06895-125

$T_A = 25^\circ\text{C}$, unless otherwise noted.

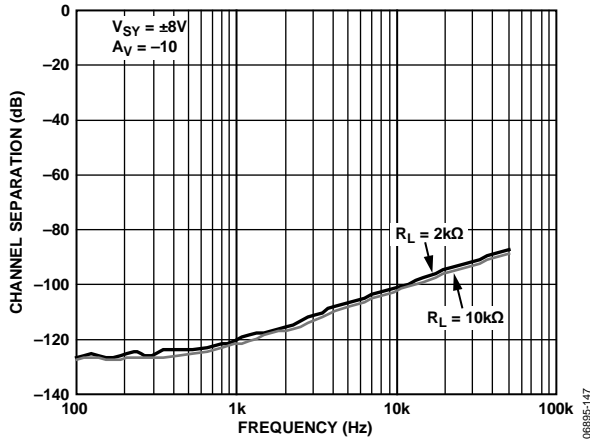


Figure 47. Channel Separation vs. Frequency

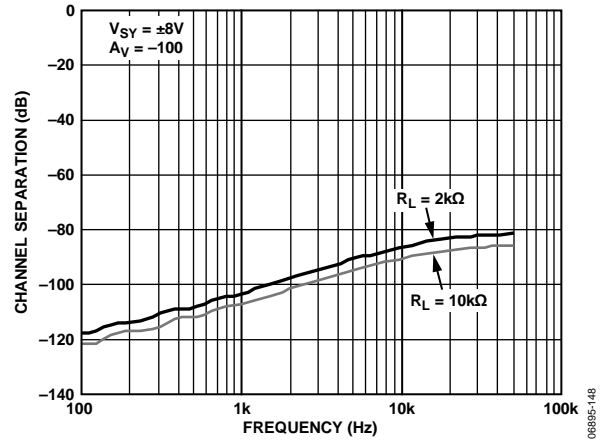


Figure 50. Channel Separation vs. Frequency

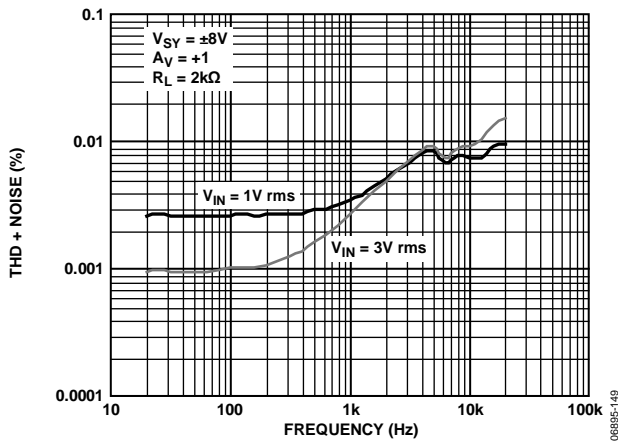


Figure 48. THD + Noise vs. Frequency

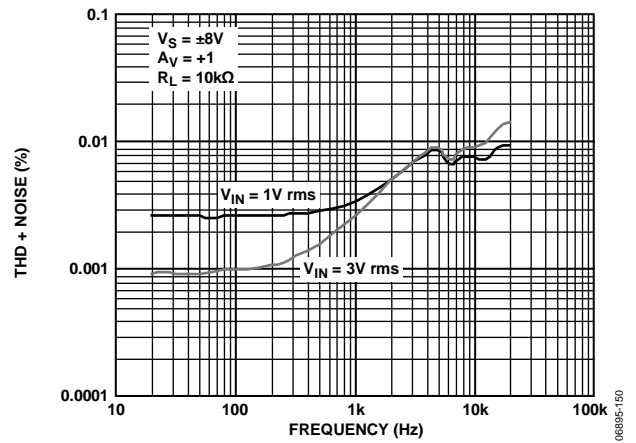


Figure 51. THD + Noise vs. Frequency

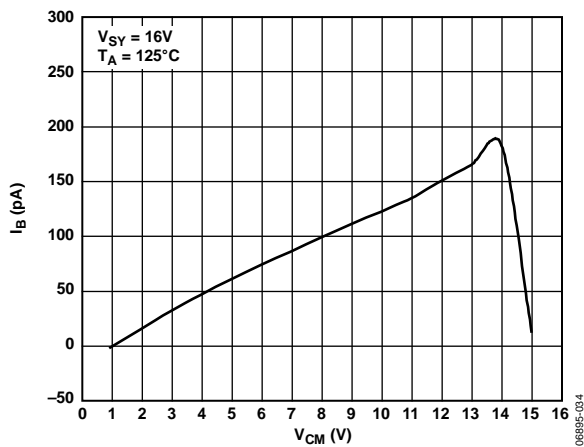


Figure 49. Input Bias Current vs. Input Common-Mode Voltage

THEORY OF OPERATION

The AD8638/AD8639 are single-supply and dual-supply, ultrahigh precision, rail-to-rail output operational amplifiers. The typical offset voltage of 3 μV allows the amplifiers to be easily configured for high gains without risk of excessive output voltage errors. The extremely small temperature drift of 30 $\text{nV}/^\circ\text{C}$ ensures a minimum offset voltage error over the entire temperature range of -40°C to $+125^\circ\text{C}$, making the amplifiers ideal for a variety of sensitive measurement applications in harsh operating environments.

The AD8638/AD8639 achieve a high degree of precision through a patented auto-zeroing topology. This unique topology allows the AD8638/AD8639 to maintain low offset voltage over a wide temperature range and over the operating lifetime. The AD8638/AD8639 also optimize the noise and bandwidth over previous generations of auto-zero amplifiers, offering the lowest voltage noise of any auto-zero amplifier by more than 50%.

Previous designs used either auto-zeroing or chopping to add precision to the specifications of an amplifier. Auto-zeroing results in low noise energy at the auto-zeroing frequency, at the expense of higher low frequency noise due to aliasing of wide-band noise into the auto-zeroed frequency band. Chopping results in lower low frequency noise at the expense of larger noise energy at the chopping frequency. The AD8638/AD8639 use both auto-zeroing and chopping in a patented ping-pong arrangement to obtain lower low frequency noise together with lower energy at the chopping and auto-zeroing frequencies, maximizing the SNR for the majority of applications without the need for additional filtering. The relatively high clock frequency of 15 kHz simplifies filter requirements for a wide, useful, noise-free bandwidth.

The AD8638 is among the few auto-zero amplifiers offered in the 5-lead SOT-23 package. This provides significant improvement over the ac parameters of previous auto-zero amplifiers. The AD8638/AD8639 have low noise over a relatively wide bandwidth (0 Hz to 10 kHz) and can be used where the highest dc precision is required. In systems with signal bandwidths ranging from 5 kHz to 10 kHz, the AD8638/AD8639 provide true 16-bit accuracy, making this device the best choice for very high resolution systems.

1/f NOISE

1/f noise, also known as pink noise, is a major contributor to errors in dc-coupled measurements. This 1/f noise error term can be in the range of several microvolts or more and, when amplified by the closed-loop gain of the circuit, can show up as a large output signal. For example, when an amplifier with 5 μV p-p 1/f noise is configured for a gain of 1000, its output has 5 mV of error due to the 1/f noise. However, the AD8638/AD8639 eliminate 1/f noise internally and thus significantly reduce output errors.

The internal elimination of 1/f noise is accomplished as follows: 1/f noise appears as a slowly varying offset to AD8638/AD8639 inputs. Auto-zeroing corrects any dc or low frequency offset. Therefore, the 1/f noise component is essentially removed, leaving the AD8638/AD8639 free of 1/f noise.

INPUT VOLTAGE RANGE

The AD8638/AD8639 are not rail-to-rail input amplifiers; therefore, care is required to ensure that both inputs do not exceed the input voltage range. Under normal negative feedback operating conditions, the amplifier corrects its output to ensure that the two inputs are at the same voltage. However, if either input exceeds the input voltage range, the loop opens and large currents begin to flow through the ESD protection diodes in the amplifier.

These diodes are connected between the inputs and each supply rail to protect the input transistors against an electrostatic discharge event, and they are normally reverse-biased. However, if the input voltage exceeds the supply voltage, these ESD diodes can become forward-biased. Without current limiting, excessive amounts of current may flow through these diodes, causing permanent damage to the device. If inputs are subject to over-voltage, insert appropriate series resistors to limit the diode current to less than 10 mA maximum.

OUTPUT PHASE REVERSAL

Output phase reversal occurs in some amplifiers when the input common-mode voltage range is exceeded. As common-mode voltage is moved outside the common-mode range, the outputs of these amplifiers can suddenly jump in the opposite direction to the supply rail. This is the result of the differential input pair shutting down, causing a radical shifting of internal voltages that results in the erratic output behavior.

The AD8638/AD8639 amplifiers have been carefully designed to prevent any output phase reversal if both inputs are maintained within the specified input voltage range. If one or both inputs exceed the input voltage range but remain within the supply rails, an internal loop opens and the output varies. Therefore, the inputs should always be less than at least 2 V below the positive supply.

OVERLOAD RECOVERY TIME

Many auto-zero amplifiers are plagued by a long overload recovery time, often in milliseconds, due to the complicated settling behavior of the internal nulling loops after saturation of the outputs. The AD8638/AD8639 are designed so that internal settling occurs within two clock cycles after output saturation happens. This results in a much shorter recovery time, less than 50 μs , when compared to other auto-zero amplifiers. The wide bandwidth of the AD8638/AD8639 enhances performance when the parts are used to drive loads that inject transients into the outputs. This is a common situation when an amplifier is used to drive the input of switched capacitor ADCs.

INFRARED SENSORS

Infrared (IR) sensors, particularly thermopiles, are increasingly used in temperature measurement for applications as wide ranging as automotive climate control, human ear thermometers, home insulation analysis, and automotive repair diagnostics. The relatively small output signal of the sensor demands high gain with very low offset voltage and drift to avoid dc errors.

If interstage ac coupling is used, as shown in Figure 52, low offset and drift prevent the output of the input amplifier from drifting close to saturation. The low input bias currents generate minimal errors from the output impedance of the sensor. Similar to pressure sensors, the very low amplifier drift with time and temperature eliminates additional errors once the system is calibrated at room temperature. The low 1/f noise improves SNR for dc measurements taken over periods often exceeding one-fifth of a second.

Figure 52 shows a circuit that can amplify ac signals from 100 μV to 300 μV up to the 1 V to 3 V levels, with a gain of 10,000 for accurate analog-to-digital conversions.

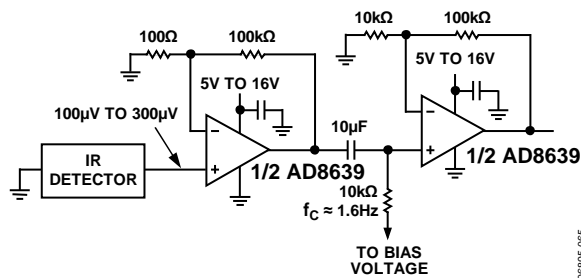


Figure 52. AD8639 Used as a Preamplifier for Thermopile

PRECISION CURRENT SHUNT SENSOR

A precision current shunt sensor benefits from the unique attributes of auto-zero amplifiers when used in a differencing configuration, as shown in Figure 53. Current shunt sensors are used in precision current sources for feedback control systems. They are also used in a variety of other applications, including battery fuel gauging, laser diode power measurement and control, torque feedback controls in electric power steering, and precision power metering.

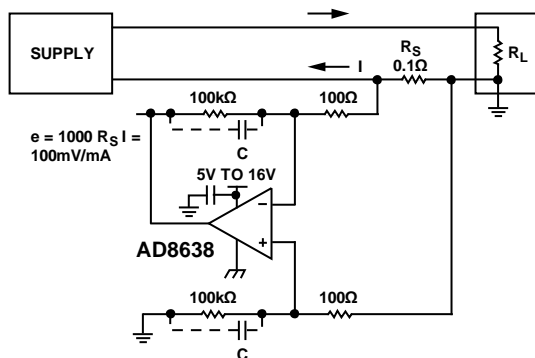


Figure 53. Low-Side Current Sensing

In such applications, it is desirable to use a shunt with very low resistance to minimize the series voltage drop; this minimizes wasted power and allows the measurement of high currents while saving power. A typical shunt may be 0.1 Ω. At measured current values of 1 A, the output signal of the shunt is hundreds of millivolts, or even volts, and amplifier error sources are not critical. However, at low measured current values in the 1 mA range, the 100 μV output voltage of the shunt demands a very low offset voltage and drift to maintain absolute accuracy. Low input bias currents are also needed to prevent injected bias current from becoming a significant percentage of the measured current. High open-loop gain, CMRR, and PSRR help to maintain the overall circuit accuracy. With the extremely high CMRR of the AD8638/AD8639, the CMRR is limited by the resistor ratio matching. As long as the rate of change of the current is not too fast, an auto-zero amplifier can be used with excellent results.

OUTPUT AMPLIFIER FOR HIGH PRECISION DACS

The AD8638/AD8639 can be used as output amplifiers for a 16-bit high precision DAC in a unipolar configuration. In this case, the selected op amp needs to have very low offset voltage (the DAC LSB is 38 μV when operating with a 2.5 V reference) to eliminate the need for output offset trims. Input bias current (typically a few tens of picoamperes) must also be very low because it generates an additional offset error when multiplied by the DAC output impedance (approximately 6 kΩ).

Rail-to-rail output provides full-scale output with very little error. Output impedance of the DAC is constant and code-independent, but the high input impedance of the AD8638/AD8639 minimizes gain errors. The wide bandwidth of the amplifier also serves well in this case. The amplifier, with a settling time of 4 μs, adds another time constant to the system, increasing the settling time of the output. For example, see Figure 54. The settling time of the AD5541 is 1 μs. The combined settling time is approximately 4.1 μs, as can be derived from the following equation:

$$t_s (TOTAL) = \sqrt{(t_s DAC)^2 + (t_s AD8638)^2}$$

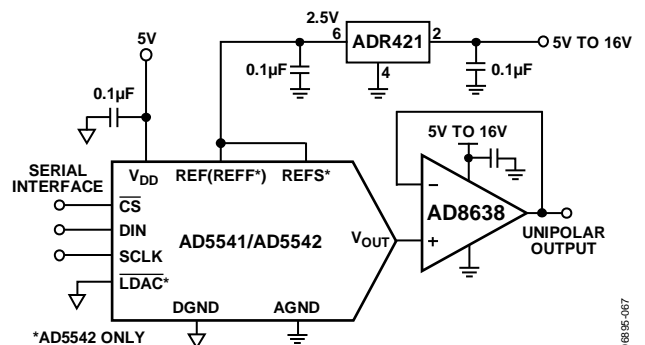
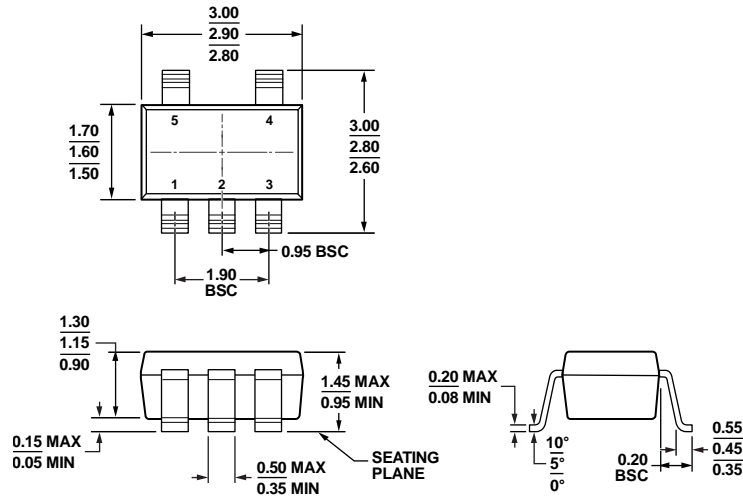


Figure 54. AD8638 Used as an Output Amplifier

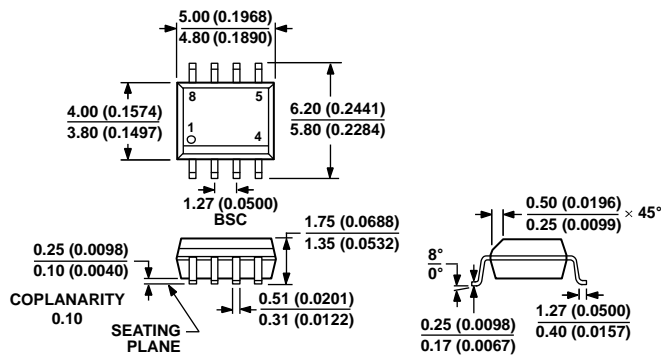
OUTLINE DIMENSIONS



COMPLIANT TO JEDEC STANDARDS MO-178-AA

Figure 55. 5-Lead Small Outline Transistor Package [SOT-23] (RJ-5)

Dimensions shown in millimeters



COMPLIANT TO JEDEC STANDARDS MS-012-AA

CONTROLLING DIMENSIONS ARE IN MILLIMETERS; INCH DIMENSIONS (IN PARENTHESES) ARE ROUNDED-OFF MILLIMETER EQUIVALENTS FOR REFERENCE ONLY AND ARE NOT APPROPRIATE FOR USE IN DESIGN.

Figure 56. 8-Lead Standard Small Outline Package [SOIC_N] Narrow Body (R-8)

Dimensions shown in millimeters and (inches)

121608-A

012407-A

AD8638/AD8639

ORDERING GUIDE

Model ^{1, 2}	Temperature Range	Package Description	Package Option	Branding
AD8638ARJZ-R2	-40°C to +125°C	5-Lead SOT-23	RJ-5	A1T
AD8638ARJZ-REEL	-40°C to +125°C	5-Lead SOT-23	RJ-5	A1T
AD8638ARJZ-REEL7	-40°C to +125°C	5-Lead SOT-23	RJ-5	A1T
AD8638ARZ	-40°C to +125°C	8-Lead SOIC_N	R-8	
AD8638ARZ-REEL	-40°C to +125°C	8-Lead SOIC_N	R-8	
AD8638ARZ-REEL7	-40°C to +125°C	8-Lead SOIC_N	R-8	
AD8639ACPZ-R2	-40°C to +125°C	8-Lead LFCSP_WD	CP-8-5	A1Y
AD8639ACPZ-REEL	-40°C to +125°C	8-Lead LFCSP_WD	CP-8-5	A1Y
AD8639ACPZ-REEL7	-40°C to +125°C	8-Lead LFCSP_WD	CP-8-5	A1Y
AD8639ARZ	-40°C to +125°C	8-Lead SOIC_N	R-8	
AD8639ARZ-REEL	-40°C to +125°C	8-Lead SOIC_N	R-8	
AD8639ARZ-REEL7	-40°C to +125°C	8-Lead SOIC_N	R-8	
AD8639ARMZ	-40°C to +125°C	8-Lead MSOP	RM-8	A1Y
AD8639ARMZ-REEL	-40°C to +125°C	8-Lead MSOP	RM-8	A1Y
AD8639ARMZ-R7	-40°C to +125°C	8-Lead MSOP	RM-8	A1Y
AD8639WARZ	-40°C to +125°C	8-Lead SOIC_N	R-8	
AD8639WARZ-RL	-40°C to +125°C	8-Lead SOIC_N	R-8	
AD8639WARZ-R7	-40°C to +125°C	8-Lead SOIC_N	R-8	

¹ Z = RoHS Compliant Part.

² W = Qualified for Automotive Applications.

AUTOMOTIVE PRODUCTS

The AD8639W models are available with controlled manufacturing to support the quality and reliability requirements of automotive applications. Note that these automotive models may have specifications that differ from the commercial models; therefore, designers should review the Specifications section of this data sheet carefully. Only the automotive grade products shown are available for use in automotive applications. Contact your local Analog Devices account representative for specific product ordering information and to obtain the specific Automotive Reliability reports for these models.

NOTES

NOTES

Mouser Electronics

Authorized Distributor

Click to View Pricing, Inventory, Delivery & Lifecycle Information:

[Analog Devices Inc.:](#)

[AD8638ARJZ-R2](#) [AD8638ARJZ-REEL7](#) [AD8638ARZ](#) [AD8639ARMZ](#) [AD8639ARZ](#) [AD8638ARJZ-REEL](#)
[AD8638ARZ-REEL](#) [AD8638ARZ-REEL7](#) [AD8639ACPZ-R2](#) [AD8639ACPZ-REEL](#) [AD8639ACPZ-REEL7](#)
[AD8639ARMZ-R7](#) [AD8639ARMZ-REEL](#) [AD8639ARZ-REEL](#) [AD8639ARZ-REEL7](#) [AD8639WARZ](#) [AD8639WARZ-R7](#)
[AD8639WARZ-RL](#)